Evaluation of cation exchange membrane performance under exposure to high Hg^0 and $HgBr_2$ concentrations

Matthieu B. Miller[1], Sarrah M. Dunham-Cheatham[2], Mae Sexauer Gustin[2], Grant C. Edwards[1,†]

[1]Department of Environmental Sciences, Macquarie University, Sydney, NSW, 2109, Australia

[2]Department of Natural Resources and Environmental Science, University of Nevada, Reno NV, 89557, United States

[†]Deceased 10 September 2018

Correspondence to: Mae Sexauer Gustin mgustin@cabnr.unr.edu

Abstract

Reactive mercury (RM), the sum of both gaseous oxidized Hg and particulate bound Hg, is an important component of the global atmospheric mercury cycle, but measurement currently depends on un-calibrated operationally-defined methods with large uncertainty and demonstrated interferences and artifacts. Cation exchange membranes (CEM) provide a promising alternative methodology for quantification of RM, but method validation and improvements are ongoing. For the CEM material to be reliable, uptake of gaseous elemental mercury (GEM) must be negligible under all conditions, and RM compounds must be captured and retained with high efficiency. In this study, the performance of CEM material under exposure to high concentrations of GEM (1.43×10^6 to 1.85×10^6 pg m^{-3}) and reactive gaseous mercury bromide ($HgBr_2$ ~ 5000 pg m^{-3}) was explored, using a custom-built mercury vapor permeation system. Quantification of total permeated Hg was measured via pyrolysis at 600 °C and detection using a Tekran® 2537A. Permeation tests were conducted for 24 to 72 hours in clean laboratory air, with absolute humidity levels ranging from 0.1 to 10 g m^{-3} water vapor. GEM uptake by the CEM material averaged no more than 0.004% of total exposure for all test conditions, which equates to a non-detectable GEM artifact for typical ambient air sample concentrations. Recovery of $HgBr_2$ on CEM filters was on average 127% compared to calculated total permeated $HgBr_2$ based on the downstream Tekran® 2537A data. The low $HgBr_2$ breakthrough on the downstream CEMs

(<1%) suggest that the elevated recoveries are more likely related to sub-optimal pyrolyzer conditions or inefficient collection on the Tekran® 2537A gold traps.

1 Introduction

Mercury (Hg) is a persistent environmental contaminant with a significant atmospheric life time, and the form and chemistry of Hg is an important determinant of its biogeochemical cycling. Mercury in the atmosphere is found in three forms: gaseous elemental mercury (GEM), gaseous oxidized mercury (GOM), and particulate bound mercury (PBM). PBM and GOM are often quantified together as reactive mercury (RM = GOM + PBM); while the term RM dilutes some specific information regarding the state of GOM in the atmosphere, it removes some uncertainty as to whether or not PBM contributes to the Hg collected by the CEMs. Atmospheric GEM, at an average global background concentration of 1 to 2 ng m^{-3}, can be reliably measured with calibrated analytical instruments (Gustin et al., 2015; Slemr et al., 2015). The measurement of GOM and PBM requires detection at part per quadrillion (pg m^{-3}) concentrations, and depends currently on un-calibrated operationally defined methods with demonstrated interferences and artifacts, and concomitant large uncertainty (Marusczak et al., 2017; Jaffe et al. 2014; McClure et al. 2014; Gustin et al. 2013; Lyman et al. 2010). Recent reviews (Zhang et al., 2017; Gustin et al., 2015) detail the shortcomings, difficulties, developments, and ongoing improvements needed for atmospheric RM measurements.

One alternative methodology that may provide improved measurement of ambient RM involves use of cation exchange membranes (CEM). CEM materials have been used to selectively measure GOM concentrations in ambient air in previous studies (Huang et al., 2017; Marusczak et al., 2017; Pierce and Gustin, 2017; Huang and Gustin, 2015a; Huang et al., 2013; Sheu and Mason, 2001; Ebinghaus et al., 1999; Mason et al., 1997; Bloom et al., 1996). Use of CEM type

54 filters (then manufactured by Gelman Sciences and referred to as “ion exchange membranes”)
55 for this purpose was first documented in the literature in a conference presentation (Bloom et al.,
56 1996), though these had also been deployed in an earlier field-based international comparative
57 study of RM measurement techniques in September, 1995 (Ebinghaus et al., 1999). In the
58 comparative study, one participating lab deployed a series of ion exchange membranes (for
59 GOM) behind a quartz fiber filter (for PBM) at a sample flow rate of 9 to 10 Lpm, for 24 h
60 measurements (filter pore sizes were not reported). Results for PBM and GOM were in similar
61 ranges of 4.5 to 26 pg m^{-3} and 13 to 23 pg m^{-3} , respectively (Ebinghaus et al., 1999).

62 The ion exchange membrane method was also applied in a 1995-96 field campaign for
63 determining the speciation of atmospheric Hg in the Chesapeake Bay area (Mason et al., 1997).
64 This study used a 5-stage Teflon filter pack system that included one up front quartz fiber filter
65 (0.8 μm pore size) to remove particles, and four downstream Gelman ion exchange membranes
66 (pore size not reported) to 1) capture GOM, 2) capture GOM breakthrough, 3) serve as
67 deployment blanks, and 4) isolate the filter train on the downstream side (Mason et al., 1997).
68 Concentrations of GOM were reported to be 5-10 pg m^{-3}, essentially at or below the method
69 detection limit and it was speculated that even this small amount may have been an artifact from
70 fine particulate Hg passing through the 0.8 μm quartz fiber filter (Mason et al., 1997). These low
71 concentrations are likely due to GOM being degraded on the quartz fiber filter or inefficient
72 uptake by the Gelman filter (see Supplemental Information Gustin et al. 2013). The 3rd-in-series
73 ion exchange membrane blanks were reported to be not significantly different in Hg
74 concentration from unused membrane material, indicating that breakthrough was not a
75 phenomenon that extended past the second ion exchange filter position.

76 The particulate Hg artifact problem was subsequently elaborated on in a further comparative
77 study focusing exclusively on RM measurement techniques (Sheu and Mason, 2001). Specific

concerns included physical particle breakthrough, re-evolution of gas-phase Hg^{2+} from PBM captured on the upstream particulate filters passing downstream to the ion exchange membranes, possible adsorption of GOM compounds to the particulate filters, or a GEM collection artifact on the ion exchange membranes. None of these concerns were proven or disproven conclusively.

Recent CEM based sampling systems typically deploy a pair of CEM disc filters without a pre-particulate filter, in replicates of 2 to 3 at a flow rate of 1.0 Lpm (Gustin et al., 2016). Each pair of filters constitutes one sample, the first filter serving as the primary RM collection surface, and the second filter capturing breakthrough. Filters are deployed for 1 to 2 weeks and then collected for analysis (Huang et al., 2017). The CEM material consists of a negatively charged polyethersulfone coated matrix (Pall Corporation), and at least one manufacturing evolution has occurred (Huang and Gustin, 2015b). Prior CEM material versions (I.C.E. 450) had a pore size of 0.45 μm, while the current CEM material (Mustang® S) has a manufacturer reported pore size of 0.8 μm.

Previous work with the I.C.E 450 material indicated it does not adsorb significant quantities of GEM in passive exposures, but selectively uptakes gas-phase Hg^{2+} species (Lyman et al., 2007). The CEM material was subsequently adapted for use in active sample flow systems, with the presumption of continued inertness to GEM and selectivity for GOM (Huang and Gustin, 2015a; Huang et al., 2013). These studies and others (Lyman et al., 2016) have shown better GOM recovery on CEM material compared to potassium chloride (KCl) coated denuder methods.

Despite these tests, the transparency of the CEM material to GEM uptake has not been conclusively demonstrated for active sampling flow rates, nor for high GEM concentrations, though limited data using low concentration manual Hg^0 injections through CEM filters suggests little or no GEM uptake (Lyman et al., 2016). However, even small rates of GEM uptake by the

CEM material could result in a significant measurement artifact (e.g. a modest 1 to 2% GEM uptake could easily overwhelm detection of typical ambient GOM concentrations). It is therefore important that a GEM artifact be ruled out if the CEM material is to be successfully deployed for ambient RM measurements.

Additionally, previous studies observed significant amounts of "breakthrough" GOM on the secondary filter. The amount of breakthrough is not consistent, neither as a constant mass, with total Hg ranging from zero to as high as 400 pg (Huang et al., 2017), nor as a percentage of Hg collected on the primary filter, ranging from 0 to 40% (Pierce and Gustin, 2017). Similar variable breakthrough issues were observed in the earliest field-based CEM measurements as well (Mason et al., 1997). In contrast to ambient measurements, previous laboratory experiments have reported only minor (0 to 16%) or no breakthrough Huang and Gustin, 2015a; Huang et al., 2013). Limited experimental work with flow rates of 1.0 and 16.7 Lpm in ambient air could not provide an explanation for differing breakthrough rates (Pierce and Gustin, 2017).

In this research we investigated the potential for GEM uptake on CEM material using a custom-built permeation system. Tests were done to investigate the ability of a pyrolyzer to convert GEM to GOM. In addition, the ability of the CEM material to capture and retain a representative GOM compound (mercury(II) bromide, $HgBr_2$) was explored, and the collection efficiency for this compound was estimated. We attempted to explain or rule out possible mechanisms of RM breakthrough for both dry and humid conditions.

2 Methods

2.1 System for sampling configuration

A Tekran® 2537A ambient mercury analyzer was integrated with a custom-built permeation system designed to enable controlled exposures of GEM and GOM to CEM filters (Fig. 1). The 2537A analyzer was calibrated at the beginning and periodically throughout the study and checked for accuracy by manual Hg^0 injections (mean recovery 101.1% ± 4.3, n = 10, SI Fig. 1). The entire system was checked for Hg contamination in clean air prior to permeation tests, and periodically during sampling (SI Fig. 2). See SI for additional information on Tekran quality control. All tubing and connections used in the permeation system were polytetrafluoroethylene (PTFE), except for the quartz glass pyrolyzer tube and perfluoroalkoxy (PFA) filter holders. Given its reactive nature, some GOM inevitably adsorbs to internal line surfaces, but the capacity of these materials to sorb and retain GOM is not infinite and a steady state of adsorption/desorption is expected after 5-6 hours of exposure to a stable concentration (Xiao et al., 1997; Gustin et al., 2013).

Sample flow through the system was alternated between two PTFE sample lines (designated Line 0 and Line 1) using a Tekran® Automated Dual Switching (TADS) unit. Sample air was constantly pulled through each line at 1.0 Lpm by the internal pump and mass flow controller (MFC) in the 2537A, or by an external flush pump (KNF Laboport® N86 KNP) and MFC (Sierra Smart-Trak® 2). Laboratory air was pulled through a single inlet at the combined rate of 2.0 Lpm, passing through a 0.2 µm PTFE particulate filter and an activated charcoal scrubber (granular activated carbon 6-12 mesh, FisherChemical®) to produce clean sample air. Additionally, for dry air permeations sample air was pulled through a Tekran® 1102 Air Dryer installed upstream of the particulate filter, and for elevated humidity permeations sample air was

pulled through the headspace of a distilled water bath (DIW, < 0.2 ng L^{-1} total Hg) that was located upstream from the charcoal scrubber to eliminate the DIW being a potential Hg source to the system. Temperature and relative humidity (RH) were measured in-line (Campbell Scientific CS215) and used for calculation of absolute humidity.

Pure liquid Hg^0 and crystalline $HgBr_2$ (purity > 99.998% Sigma-Aldrich®) were used as Hg vapor sources. The elemental Hg^0 bead was contained in a PTFE vial. Solid $HgBr_2$ crystals were packed in thin-walled PTFE heat-shrink tubing (O.D. 0.635 cm) with solid Teflon plugs in both ends to create a permeation tube with an active permeation length of 2 mm (Huang et al., 2013). The $HgBr_2$ permeation tube was also placed in the bottom of a PTFE vial, and the permeation vials were submerged in a temperature-controlled laboratory chiller (0.06 ± 0.13 °C, Cole Parmer Polystat®). A low source temperature was favored, because higher temperatures would have produced unacceptably high concentrations, and there is evidence that at higher temperatures a small amount of Hg^0 can be evolved from Hg^{2+} compounds (Xiao et al., 1997).

An ultra-high purity nitrogen (N_2) carrier gas was passed through the permeation vials at 0.2 Lpm to carry the target Hg vapor into the main sample line through a PTFE T-junction. The main sample line was split into Line 0 and Line 1 immediately downstream from the permeation flow junction, with flow on each line controlled by MFC. Line 0 proceeded directly to the 2537A without modification during GEM permeations (Fig. 1A), but housed CEM filters during the $HgBr_2$ permeations (Fig. 1B, 1C). Line 1 contained an in-line pyrolyzer unit. The goal of the pyrolyzer was to convert all Hg to GEM for detection on the Tekran® 2537A.

2.2 Pyrolyzer

The pyrolyzer used in the study (SI Fig. 3) consisted of a 25.4 cm long quartz glass tube of 0.625 cm diameter (custom, URG Corporation). A loosely packed 3 cm section of quartz wool was

lodged in the mid-section of the tube, and this 3 cm section was wrapped with 22 gauge Nichrome wire (18 loops). The quartz tube was closely contained within 2.5 cm thick quartz fiber insulation within a 1.6 mm aluminum casing, except for an enclosed air space around the heated Nichrome coil section. The coil wire was connected to 16 AWG stranded copper wire with all metal disconnects that were buried within the quartz fiber insulation to reduce thermal fatigue on the connections. The copper wire insulation was stripped and replaced with higher temperature heat-shrink insulation where the wiring passed through the pyrolyzer case to the external power supply. The tip of a 150 mm long K-type thermocouple (Auber WRNK-191) was inserted through the insulation into the heated air space next to the coil to provide a temperature feedback for a PID controller (Auber SYL-1512A). Power to the Nichrome coil was supplied by a 12 VDC transformer through a solid-state relay (Auber MGR-1D4825) switched by the PID controller. It was found that the position of the feedback thermocouple in the airspace outside of the heating coil caused a large discrepancy between nominal temperature setpoint and actual temperature inside the heated section of pyrolyzer tube. In general, much higher temperatures are achieved inside the coil than outside. To compensate for this, actual temperature at the heated coil section was verified to 600°C by external IR sensor and internal thermocouple probe.

To test if higher pyrolyzer temperatures converted more GOM to GEM for detection by the Tekran 2537, the pyrolyzer temperature was increased to 650, 800, and 1,000ºC (SI Fig. 4). Pyrolyzer temperatures were measured by placing a thermocouple inside the pyrolyzer. GOM concentrations measured as GEM by the Tekran 2537A increased at 600 and 800ºC relative to 375ºC. There was no significant difference between the amount of mercury concentrations in the downstream Tekran 2537A when the pyrolyzer was at 600 and 800ºC C (*t-test, $p = 0.08$*), indicating that the increased pyrolyzer temperature did not convert more GOM to GEM. However, when the pyrolyzer temperature was increased to 1000 ºC, significantly more mercury

was measured by the downstream Tekran 2537A relative to when the pyrolyzer was at 650ºC (*t-test, p = 0.00*), indicating that the higher temperature was more efficient at converting GOM to GEM; however, the pyrolyzer design could not sustain the 1000 ºC temperature and was deemed unsafe to use in the experimental permeation system. Thus, all experiments were performed with a pyrolyzer temperature of 600ºC.

The residence time in the pyrolyzer tube was approximately 1.5 seconds. Quartz wool was added to increase the amount of surface area available to facilitate reactions and maximize the amount of GOM converted to GEM in the pyrolyzer. Based on supplemental experiments, the downstream Tekran® 2537A Hg measurements when the pyrolyzer was at 650 ºC was 75% compared to the measurements when the pyrolyzer was at 1000 ºC (SI Fig. 4), indicating a higher GOM to GEM conversion efficiency with higher pyrolyzer temperatures. Though this conversion efficiency value does not describe the exact inefficiency of the experimental system in this study, it provides an estimate for the efficiency of the pyrolyzer design in this study. Having an efficient pyrolyzer provides us with a means of constraining permeation tube permeation rates.

2.3 Sample deployment

CEM filters were deployed in 2-stage, 47 mm disc PFA filter holders (Savillex©). The primary "A" filter in the 2-stage holder is the first to be exposed to the permeated Hg, with the secondary "B" filter mounted immediately behind the A filter (A to B distance ~ 3mm) to measure potential breakthrough. For GEM permeations, three 2-stage filter holders were placed in-series on Line 1 behind the pyrolyzer unit (Fig. 1A), while total Hg coming through the system was measured on Line 0 with no filters in place. This allowed simultaneous exposure of 6 CEM filters in one GEM sample exposure. The first CEM filter in-line served to scrub any small residual RM passing through the system and pyrolyzer, and these first in-line filters were removed for the calculations

of mean GEM uptake rate, (SI. 5 and discussion). A controlled experiment was also performed to ensure that both Lines 0 and 1 were conducting comparable concentrations of mercury under the experimental conditions. Two-stage filter packs were deployed with CEM filters in each line at equal distances from the permeation tube. The membranes were deployed for the same amount of time in triplicate and analyzed to quantify the amount of total mercury sorbed to the membranes. The average % deviation between lines was 2.9%, with a maximum deviation of 5.4%. These results indicated that though there may be some difference in the amount of mercury passing through Lines 0 and 1, the difference was relatively small.

For determining the potential for GOM breakthrough, two system configurations were used. In the first configuration (Fig. 1B), the total Hg concentration of air that passed through the pyrolyzer on Line 1 was measured without any filters, while Line 0 held one 2-stage CEM filter pair for $HgBr_2$ loading. This configuration allowed for 10 min interval quantification of the $HgBr_2$ permeation concentration through Line 1 using the 2537A, and comparison with total Hg loading on the CEM filters on Line 0.

In the second configuration, replicate filters were concurrently loaded with $HgBr_2$ by placing 2-stage CEM filter holders on both Line 0 and Line 1 (upstream of the pyrolyzer, Fig. 1C). In all $HgBr_2$ exposures, the filter holders were placed as close to the permeation vial as possible, with a total distance from vial to filter surface of approximately 20 cm. Mercury bromide permeation was conducted in dry air and elevated humidity air. The difference between one line being fully open to the $HgBr_2$ permeation flow (configuration Fig. 1B) and then closed by deployment of the CEM filters (configuration Fig. 1C) enabled a rough determination of the amount of $HgBr_2$ line-loss within the system.

2.4 Analyses of cation exchange membranes

After permeation, CEM filters were collected into clean, sterile polypropylene vials and analyzed for total Hg by digestion in an oxidizing acid solution, reduction to Hg^0, gold amalgamation, and final quantification by cold vapor atomic fluorescence spectrometry (CVAFS, EPA Method 1631, Rev. E) using a Tekran® 2600 system. The system background Hg signal was determined for every analytical run by analyzing pure reagent solution in the same vials and at the same volume as used for actual filter samples. Total Hg standards (5 to 100 ppb) were analyzed before and after each batch of 10 filter samples to check precision and recovery, and the mean recovery for all Hg standards was 97.2 ± 5.0 % (n = 37). Analysis for total Hg on the CEM filters provided for comparison of total Hg filter loading, and verification of in-line results. A to B filter breakthrough was calculated by comparison of total Hg recoveries on the primary and secondary CEM filters, using Eq. (1):

$$\% \, Breakthrough = 100 * CEM_{2nd}/(CEM_{1st} + CEM_{2nd}) \quad (1)$$

Blank CEM filters were collected and analyzed in the same manner with every set of sample filters deployed on the permeation system, and the overall mean filter blank value was subtracted from all total Hg values to calculate the final blank-corrected Hg values used for data analysis. All data were analyzed in Microsoft® Excel (version 16.12) and RStudio® (version 3.2.2).

3 Results

3.1 Elemental Mercury Uptake on CEM Filters

Elemental Hg uptake on CEM material was negligible for permeated Hg^0 vapor concentrations ranging from 1.43×10^6 to 1.85×10^6 pg m^{-3} (Fig. 2). High GEM concentrations were employed in

this study under the logic that if no GEM uptake was observed at high concentrations, a similar lack of GEM uptake can be expected for lower concentrations.

The mean Hg mass on blank CEM filters was 50 ± 20 pg (n = 28). For permeations into dry sample air of 0.5 ± 0.1 g m^{-3} water vapor (WV), total mean Hg^0 permeation exposures of 2.7×10^6 pg (24 h) and 7.3×10^6 pg (72 h) resulted in total (blank-corrected) Hg recoveries on the CEM filters of 100 ± 40 pg (n = 10) and 280 ± 110 pg (n = 5), respectively. These quantities of total recovered Hg equate to a mean GEM uptake rate on the CEM filters of 0.004 ± 0.002% (0.006 ± 0.006% including first in-line filter). For GEM permeations into ambient humidity sample air (2 to 4 g m^{-3} WV), at a slightly lower total mean permeated Hg^0 24 h exposure of 2.1×10^6 pg, total (blank-corrected) Hg recoveries on the CEM filters were 55 ± 30 pg (n =10), equating to a GEM uptake rate of 0.003 ± 0.001% (0.005 ± 0.005% including first in-line filter).

The first CEM filter in-line during the GEM permeations always showed more total Hg than the following 5 downstream filters that were not significantly different from each other (SI Fig. 5). It is unlikely that the Hg observed on the first CEM filters resulted from GEM uptake. Even at the highest GEM permeation rate, the first filter captured only ~1700 pg of Hg, out of a total permeated amount of over 7.3 *million* pg (a 0.02 % uptake rate). This means that the downstream CEM filters were still exposed to about 7.2985 *million* pg of GEM but captured less total Hg. As we cannot entirely rule out the possibility of some small rate of *in-situ* oxidation of GEM in the system, at the surface of the Hg^0 bead or in the vapor phase, the first in-line filters were not included in the calculation of GEM uptake rates because of suspicion that some component of the Hg captured on the first filter was GOM. The overall GEM uptake rate was linear (r^2 = 0.69, p = 0.00; SI Fig. 5) for the range of concentrations used in this study, indicating a similar low uptake rate can be expected down to lower GEM concentrations. GEM uptake by first in-line

284 filters was also linear (r^2 = 0.92, p = 0.00), though these results are based on 5 data points.
285 Exponential models poorly fit the experimental data for both the overall GEM uptake and uptake
286 by first in-line filters (SI Fig. 5).

287 **3.2 Mercury Bromide Uptake on CEM Filters**

288 Breakthrough of $HgBr_2$ vapor from the primary (A) to secondary (B) CEM filters was low for all
289 conditions tested in this study (Table 1). These conditions included $HgBr_2$ permeated into clean
290 dry laboratory air with < 0.5 g m^{-3} WV, clean air at ambient room humidity (4 to 5 g m^{-3} WV),
291 and clean air at elevated humidity (10 to 11 g m^{-3} WV), at line temperatures between 17 to 19
292 °C. Overall, the mean A to B filter breakthrough ranged from 0 to 0.5%, and averaged 0.2 ± 0.2
293 % (n = 17), with no statistical difference observed in mean breakthrough rates for the three levels
294 of humidity (ANOVA, p = 0.124).

295 The first $HgBr_2$ permeation in clean dry (< 0.5 g m^{-3} WV) laboratory air was over a 96 h period,
296 using the system configuration in Fig. 1B to establish an approximate permeation rate (Fig. 3).
297 Total Hg reaching the 2537A through the pyrolyzer on Line 1 (red line, Fig. 3) indicated an
298 average $HgBr_2$ exposure concentration of 4540 pg m^{-3}, or about 4.5 pg min^{-1} from the permeation
299 tube. This permeated concentration of $HgBr_2$ was deliberately much higher than ambient in order
300 to test retention and break through at high levels. It should be noted that these concentrations are
301 50 – 1000 times above background ambient concentrations and the performance of the CEM
302 filters at low concentrations could be slightly different. After this permeation, total blank-
303 corrected $HgBr_2$ loading on the primary CEM filter on Line 0 was 49400 pg, but only 50 pg on
304 the secondary CEM filter, indicating a breakthrough rate of approximately 0.1%. Total Hg
305 reaching the 2537A through the CEM filters on Line 0 (black line, Fig. 3) over this time period
306 was 15 pg, mostly at the beginning of the deployment when some ambient Hg entered the

opened system. The low concentrations of Hg measured downstream in Line 0 on the 2537A corroborates that breakthrough of $HgBr_2$ was low. These data also demonstrate that the CEM material did not saturate with a $HgBr_2$ loading of ~ 50000 pg, a loading far higher than could be expected in ambient conditions.

Subsequent replicate 24 h $HgBr_2$ permeations in clean dry air resulted in consistent total Hg loading on CEM filters placed on both lines concurrently (8560 ± 320 pg, n = 6, Samples 2-7 Table 1), and mean total Hg on the secondary CEM filters was 20 ± 10 pg (average breakthrough of 0.3%). On Line 0 (black line, Fig.3), which was never open to $HgBr_2$ vapor downstream from the CEM filters at any point in the study, Hg measured at the 2537A was zero for all three 24 h permeations, indicating no breakthrough (Samples 2, 4, & 6, Table 1). However, on Line 1 that had been exposed to the full $HgBr_2$ vapor concentration of 4540 pg m^{-3} over the duration of the 96 h permeation test, 1155 pg of Hg were measured downstream in the first 24 h sample (Sample 3, Table 1). The amount of downstream Hg dropped to 10 pg in the second 24 h, and 6 pg in the third 24 h (Samples 5 & 7, Table 1). This downstream Hg in Line 1 (compared to the zero Hg simultaneously observed on Line 0) is attributed to volatilization of $HgBr_2$ that had adsorbed to the line material during the open permeation flow. At the moment CEM filters were deployed on Line 1 (red-to-blue transition, Fig. 3), a rapid asymptotic decline in the Hg signal began. This decay curve supports drawdown and depletion of a Hg reservoir on the interior line surfaces behind the CEM filters, and not a continuous source such as breakthrough from the permeation tube that was still supplying $HgBr_2$ to both sample lines. The total mass of Hg volatized from the interior line surfaces (1155 pg) represents 4 to 5% of the total $HgBr_2$ that had passed through Line 1 (~25000 pg based on 2537A measurement). Eventually, Hg reaching the 2537A through Line 1 decreased to zero during the same 24 h filter deployment, indicating the majority of $HgBr_2$ line contamination in a high-concentration

permeation system can be expected to flush out within ~12 h. However, we caution that materials used in high-concentration permeation systems, despite being flushed out, should not be used for background ambient air work without at least a very thorough acid cleaning.

Additional $HgBr_2$ permeations were made at two levels of in-line humidity. At ambient room humidity (4 to 5 g m^{-3} WV), mean total Hg measured on the CEM filters was 7910 ± 520 pg (n = 4; Samples H2-5, Table 1), with an average breakthrough to the secondary filters of 0.3%. When normalized for sample volume, the mean $HgBr_2$ loading on CEM filters during ambient humidity (5968 ± 125 pg) and dry air (5995 ± 188 pg) permeations was not statistically significantly different (t-test $p = 0.790$). $HgBr_2$ breakthrough rates were also the same (0.3%) as during the dry air permeations, indicating that the permeation system was operating similarly at the two humidity levels, and suggesting that absolute humidity concentrations of 4 to 5 g m^{-3} WV had insignificant effects on collection of $HgBr_2$ in clean laboratory air by the CEM material.

An increase in humidity resulted in an initial large increase in Hg measured at the 2537A downstream of the CEM filters on Line 0 (Sample H1, Table 1), concurrently with an open $HgBr_2$ permeation flow through Line 1 while both lines were subjected to increased RH. This downstream Hg on Line 0 dropped substantially to zero in ~10 h in the first 24 h deployment (Sample H2, Table 1), and was zero for the duration of the second 24 h deployment (Sample H4, Table 1). Hg rapidly declined to zero, due to off-gassing from the tubing induced by the increased humidity, which facilitated a heterogeneous surface reduction of $HgBr_2$ to GEM in the short section of line between the permeation source and CEM filters. This phenomenon was also observed during the Reno Atmospheric Mercury Intercomparison eXperiment (RAMIX; Gustin et al., 2013). Reduced $HgBr_2$ then then passed through to the 2537A as GEM. As the breakthrough rate and the mean $HgBr_2$ loading on the CEM filters did not change between the dry air and ambient humidity permeations, the downstream Hg observed at the 2537A during the

ambient humidity permeations cannot be attributed to a loss of Hg from the CEM filters and is more likely due to a process in the sample lines.

As a further test of possible humidity effects, two replicate 24 h CEM filter deployments were conducted in elevated humidity conditions (10 to 11 g m^{-3} WV) created by an in-line water bath. Mean total Hg loading on the primary CEM filters was higher compared to the previous permeations (11700 ± 720 pg, n = 4, Samples H9-12, Table 1), indicating an increase in the effective $HgBr_2$ permeation rate, possibly due to the perturbation caused by a poor filter seal and small leak in the preceding deployment (Sample H7-8, Table 1). However, mean total Hg on the secondary CEM filters was 20 ± 20 pg, indicating an average breakthrough of 0.1%, less than the breakthrough observed for the lower humidity permeations.

4 Conclusions

GEM uptake on the CEM material was negligible under the laboratory conditions and high GEM loading rates (3 orders of magnitude above ambient) tested in this study, with an overall linear uptake rate of 0.004% (SI Fig. 5). This uptake rate would be insignificant at typical ambient atmospheric Hg concentrations (1 to 2 ng m^{-3}). As a hypothetical example, a CEM filter sampling ambient air at an average GEM concentration of 2 ng m^{-3} for a typical 2-week sample period would have a total Hg^0 exposure of ~40000 pg. At the calculated uptake rate of 0.004%, a maximum 1.6 pg of Hg observed on the sample filter could be attributed to GEM artifact. Although further work is required to more definitively determine detection and quantification limits of the various CEM methodologies, based on the mean total Hg mass of 50 ± 20 pg observed in this study, the artifact of GEM uptake by the CEMs would be below the detection

limit observed here. This corroborates the lack of GEM uptake seen by Lyman et al. (2016) for manual Hg^0 injections on CEM filters at lower total mass loadings of 300 to 6000 pg.

Mean $HgBr_2$ breakthrough from primary to secondary CEM filters averaged 0.2 ± 0.2% over all test conditions. A to B filter breakthrough was derived from a comparison between the large amount of $HgBr_2$ permeated onto the primary CEM filters, to the small amount of $HgBr_2$ that collected on the secondary CEM filters, 3 mm immediately downstream. The measurement of 1000s of pg of Hg on the primary filter, and only 10s of pg on the secondary filter, leads to the conclusion that the primary filter removed the majority of $HgBr_2$ from the sample air stream under laboratory conditions applied in this study. In addition, low breakthrough was corroborated by downstream measurement of the air stream passing through the CEM filters, using the Tekran® 2537A. The average breakthrough to the 2537A was 0 pg for 24 h permeations in dry air, and 0 to 40 pg in humid air, for filter deployments at steady-state (> 24 h without large perturbations).

While the permeation system was not specifically optimized for a quantitative mass balance between permeated $HgBr_2$ and $HgBr_2$ recovered on the CEM filters, a rough estimation of the CEM collection efficiency is possible. Using the $HgBr_2$ permeations conducted in clean dry air (mean loading 8560 pg), and comparing this to the mean Hg concentration measured at the 2537A analyzer during the last 24 h of the 96 h permeation measurement (4680 pg m^{-3} or 6739 pg per 24 h), $HgBr_2$ recovery on the CEM filters averaged 127%. Adjusting the expected permeated $HgBr_2$ mass for our estimated line-loss (~4-5%) changed the recoveries to ~123%. Still, $HgBr_2$ loading on the CEM filters was ~23% higher than expected based on the pyrolyzed total measurement on the 2537A, indicating not all $HgBr_2$ was converted to GEM. This can be explained by the pyrolyzer design used in this study not being 100% efficient at thermally

400 reducing $HgBr_2$ to Hg^0, based on the higher total Hg recoveries on the CEM filters versus total
401 Hg measured through the pyrolyzer on the Tekran 2537.

402 The technique of gold amalgamation in general, and specifically including the Tekran® 2537A
403 analyzer, is widely considered to provide a quantitative total gaseous Hg measurement, at or very
404 near 100% collection efficiency for Hg^0 and Hg compounds (Temme et al., 2003; Landis et al.,
405 2002; Schroeder et al, 1995; Dumarey et al., 1985; Schroeder and Jackson, 1985). However, to
406 our knowledge collection and desorption efficiencies on gold traps have not been demonstrated
407 for $HgBr_2$. The stated desorption temperature of the Tekran® 2537A gold traps is 500 °C, but
408 temperatures as low as 375 °C have been reported (Gustin et al., 2013). This would cause
409 reduced thermal decomposition efficiency for all captured GOM compounds, including $HgBr_2$.
410 We speculate that a combination of incomplete thermal decomposition to Hg^0 at both the 600 °C
411 pyrolyzer and during the best-case 500 °C desorption of the 2537A gold traps contributed to the
412 ~20% non-detection of total permeated $HgBr_2$ as it passed through the CVAFS optical path.
413 Evidence for this conclusion can be seen in the 134% increase in Hg collection by the Tekran®
414 2537A when the pyrolyzer was at 1000 ºC, as compared to at 650 ºC (SI Fig. 4), in
415 supplementary experiments.

416 While our results validated some basic performance metrics for the CEM material, they did not
417 provide data that could fully explain the higher levels of breakthrough observed for CEM filters
418 deployed in ambient air over the 1-to-2 week sample periods in previous studies. Increasing
419 humidity by itself did not affect observed $HgBr_2$ breakthrough. A $HgBr_2$ loading of ~50000 pg
420 also did not lead to increased breakthrough, indicating there is no saturation effect on CEM filter
421 capacity at a GOM loading far greater than expected from ambient concentrations. It remains
422 unclear, though, whether breakthrough results from different collection efficiencies for GOM
423 compounds other than $HgBr_2$, or whether breakthrough results from a degradation of GOM

retention capacity in the CEM material when exposed to ambient air chemistries not simulated in this study. Also, our experiments were conducted in particulate-free air, which leaves open the possibility that breakthrough is related to capture (or lack thereof) of PBM by the CEM material.

Further testing and refinements are necessary, beginning with optimization of the pyrolyzer parameters (e.g., temperature, volume) to allow for a more accurate quantitative comparison between the CEM and Tekran® 2537A results. Permeation rates of $HgBr_2$ were variable and need to be more precisely controlled, a standardized and stable GOM permeation system being needed in general. This study was undertaken using controlled laboratory conditions, but CEM performance needs to be further validated in ambient air. Specifically, the reasons for RM breaking through CEM filters deployed in ambient air still need to be determined.

Acknowledgements

The authors would like to acknowledge funding from Macquarie University iMQRES 2015148 and NSF Grant 629679. Valuable input and assistance were received from Dr. Ashley Pierce, Dr. Seth Lyman, and the students of Dr. Gustin's laboratory. We bid an untimely farewell to Dr. Grant C. Edwards, who was ever a cheerful friend, mentor, and colleague. Dr. Edwards passed away unexpectedly on September 10, 2018. We thank the diligent reviewers for their valuable and constructive comments.

References

Bloom, N., Prestbo, E., and VonderGeest, E.: Determination of atmospheric gaseous Hg(II) at the pg/m 3 level by collection onto cation exchange membranes, followed by dual amalgamation/cold vapor atomic fluorescence spectrometry, 4th International Conference on Mercury as a Global Pollutant, Hamburg, 1996.

Dumarey, R., Dams, R., and Hoste, J.: Comparison of the collection and desorption efficiency of activated charcoal, silver, and gold for the determination of vapor phase atmospheric mercury, Analytical Chemistry, 57, 2638-2643, 10.1021/ac00290a047, 1985.

Ebinghaus, R., Jennings, S. G., Schroeder, W. H., Berg, T., Donaghy, T., Guentzel, J., Kenny, C., Kock, H. H., Kvietkus, K., Landing, W., Muhleck, T., Munthe, J., Prestbo, E. M., Schneeberger, D., Slemr, F., Sommar, J., Urba, A., Wallschlager, D., and Xiao, Z.: International field intercomparison measurements of atmospheric mercury species at Mace Head, Ireland, Atmospheric Environment, 33, 3063-3073, 1999.

Gustin, M. S., Huang, J., Miller, M. B., Peterson, C., Jaffe, D. A., Ambrose, J., Finley, B. D., Lyman, S. N., Call, K., Talbot, R., Feddersen, D., Mao, H., and Lindberg, S. E.: Do We Understand What the Mercury Speciation Instruments Are Actually Measuring? Results of RAMIX, Environmental Science & Technology, 47, 7295-7306, 10.1021/es3039104, 2013.

Gustin, M. S., Amos, H. M., Huang, J., Miller, M. B., and Heidecorn, K.: Measuring and modeling mercury in the atmosphere: a critical review, Atmos. Chem. Phys., 15, 5697-5713, 10.5194/acp-15-5697-2015, 2015.

Gustin, M. S., Pierce, A. M., Huang, J., Miller, M. B., Holmes, H. A., and Loria-Salazar, S. M.: Evidence for Different Reactive Hg Sources and Chemical Compounds at Adjacent Valley and High Elevation Locations, Environmental Science & Technology, 50, 12225-12231, 10.1021/acs.est.6b03339, 2016.

Huang, J., Miller, M. B., Weiss-Penzias, P., and Gustin, M. S.: Comparison of Gaseous Oxidized Hg Measured by KCl-Coated Denuders, and Nylon and Cation Exchange Membranes, Environmental Science & Technology, 47, 7307-7316, 10.1021/es4012349, 2013.

Huang, J., and Gustin, M. S.: Uncertainties of Gaseous Oxidized Mercury Measurements Using KCl-Coated Denuders, Cation-Exchange Membranes, and Nylon Membranes: Humidity Influences, Environmental Science & Technology, 49, 6102-6108, 10.1021/acs.est.5b00098, 2015a.

Huang, J., and Gustin, M. S.: Use of Passive Sampling Methods and Models to Understand Sources of Mercury Deposition to High Elevation Sites in the Western United States, Environmental Science & Technology, 49, 432-441, 10.1021/es502836w, 2015b.

Huang, J., Miller, M. B., Edgerton, E., and Sexauer Gustin, M.: Deciphering potential chemical compounds of gaseous oxidized mercury in Florida, USA, Atmos. Chem. Phys., 17, 1689-1698, 10.5194/acp-17-1689-2017, 2017.

480 Jaffe, D. A., Lyman, S., Amos, H. M., Gustin, M. S., Huang, J., Selin, N. E., Levin, L., ter
481 Schure, A., Mason, R. P., Talbot, R., Rutter, A., Finley, B., Jaeglé, L., Shah, V., McClure, C.,
482 Ambrose, J., Gratz, L., Lindberg, S., Weiss-Penzias, P., Sheu, G.-R., Feddersen, D., Horvat, M.,
483 Dastoor, A., Hynes, A. J., Mao, H., Sonke, J. E., Slemr, F., Fisher, J. A., Ebinghaus, R., Zhang,
484 Y., and Edwards, G.: Progress on Understanding Atmospheric Mercury Hampered by Uncertain
485 Measurements, Environmental Science & Technology, 48, 7204-7206, 10.1021/es5026432,
486 2014.

487 Landis, M. S., Stevens, R. K., Schaedlich, F., and Prestbo, E. M.: Development and
488 characterization of an annular denuder methodology for the measurement of divalent inorganic
489 reactive gaseous mercury in ambient air, Environmental Science & Technology, 36, 3000-3009,
490 10.1021/es015887t, 2002.

491 Lyman, S., Jones, C., O'Neil, T., Allen, T., Miller, M., Gustin, M. S., Pierce, A. M., Luke, W.,
492 Ren, X., and Kelley, P.: Automated Calibration of Atmospheric Oxidized Mercury
493 Measurements, Environmental Science & Technology, 50, 12921-12927,
494 10.1021/acs.est.6b04211, 2016.

495 Lyman, S. N., Gustin, M. S., Prestbo, E. M., and Marsik, F. J.: Estimation of Dry Deposition of
496 Atmospheric Mercury in Nevada by Direct and Indirect Methods, Environmental Science &
497 Technology, 41, 1970-1976, 10.1021/es062323m, 2007.

498 Lyman, S. N., Jaffe, D. A., and Gustin, M. S.: Release of mercury halides from KCl denuders in
499 the presence of ozone, Atmospheric Chemistry and Physics, 10, 8197-8204, 10.5194/acp-10-
500 8197-2010, 2010.

501 Marusczak, N., Sonke, J. E., Fu, X., and Jiskra, M.: Tropospheric GOM at the Pic du Midi
502 Observatory—Correcting Bias in Denuder Based Observations, Environmental Science &
503 Technology, 51, 863-869, 10.1021/acs.est.6b04999, 2017.

504 Mason, R., Lawson, N., and Sullivan, K.: The concentration, speciation and sources of mercury
505 in Chesapeake Bay precipitation, Atmospheric Environment, 31, 3541-3550, 10.1016/S1352-
506 2310(97)00206-9, 1997.

507 McClure, C. D., Jaffe, D. A., and Edgerton, E. S.: Evaluation of the KCI Denuder Method for
508 Gaseous Oxidized Mercury using HgBr2 at an In-Service AMNet Site, Environmental Science &
509 Technology, 48, 11437-11444, 10.1021/es502545k, 2014.

510 Pierce, A. M., and Gustin, M. S.: Development of a Particulate Mass Measurement System for
511 Quantification of Ambient Reactive Mercury, Environmental Science & Technology, 51, 436-
512 445, 10.1021/acs.est.6b04707, 2017.

513 Schroeder, W., and Jackson, R.: An instrumental analytical technique for speciation of
514 atmospheric mercury, International Journal of Environmental Analytical Chemistry, 22, 1-18,
515 10.1080/03067318508076405, 1985.

Schroeder, W., Keeler, G., Kock, H., Roussel, P., Schneeberger, D., and Schaedlich, F.: International field intercomparison of atmospheric mercury measurement methods, Water Air and Soil Pollution, 80, 611-620, 10.1007/BF01189713, 1995.

Sheu, G. R., and Mason, R. P.: An examination of methods for the measurements of reactive gaseous mercury in the atmosphere, Environmental Science & Technology, 35, 1209-1216, 10.1021/es001183s, 2001.

Slemr, F., Angot, H., Dommergue, A., Magand, O., Barret, M., Weigelt, A., Ebinghaus, R., Brunke, E., A Pfaffhuber, K., Edwards, G., Howard, D., Powell, J., Keywood, M., and Wang, F.: Comparison of mercury concentrations measured at several sites in the Southern Hemisphere, 3125-3133 pp., 2015.

Temme, C., Einax, J. W., Ebinghaus, R., and Schroeder, W. H.: Measurements of Atmospheric Mercury Species at a Coastal Site in the Antarctic and over the South Atlantic Ocean during Polar Summer, Environmental Science & Technology, 37, 22-31, 10.1021/es025884w, 2003.

Xiao, Z., Sommar, J., Wei, S., and Lindqvist, O.: Sampling and determination of gas phase divalent mercury in the air using a KCl coated denuder, Fresenius Journal of Analytical Chemistry, 358, 386-391, 1997.

Zhang, L., Lyman, S., Mao, H., Lin, C. J., Gay, D. A., Wang, S., Sexauer Gustin, M., Feng, X., and Wania, F.: A synthesis of research needs for improving the understanding of atmospheric mercury cycling, Atmos. Chem. Phys., 17, 9133-9144, 10.5194/acp-17-9133-2017, 2017.

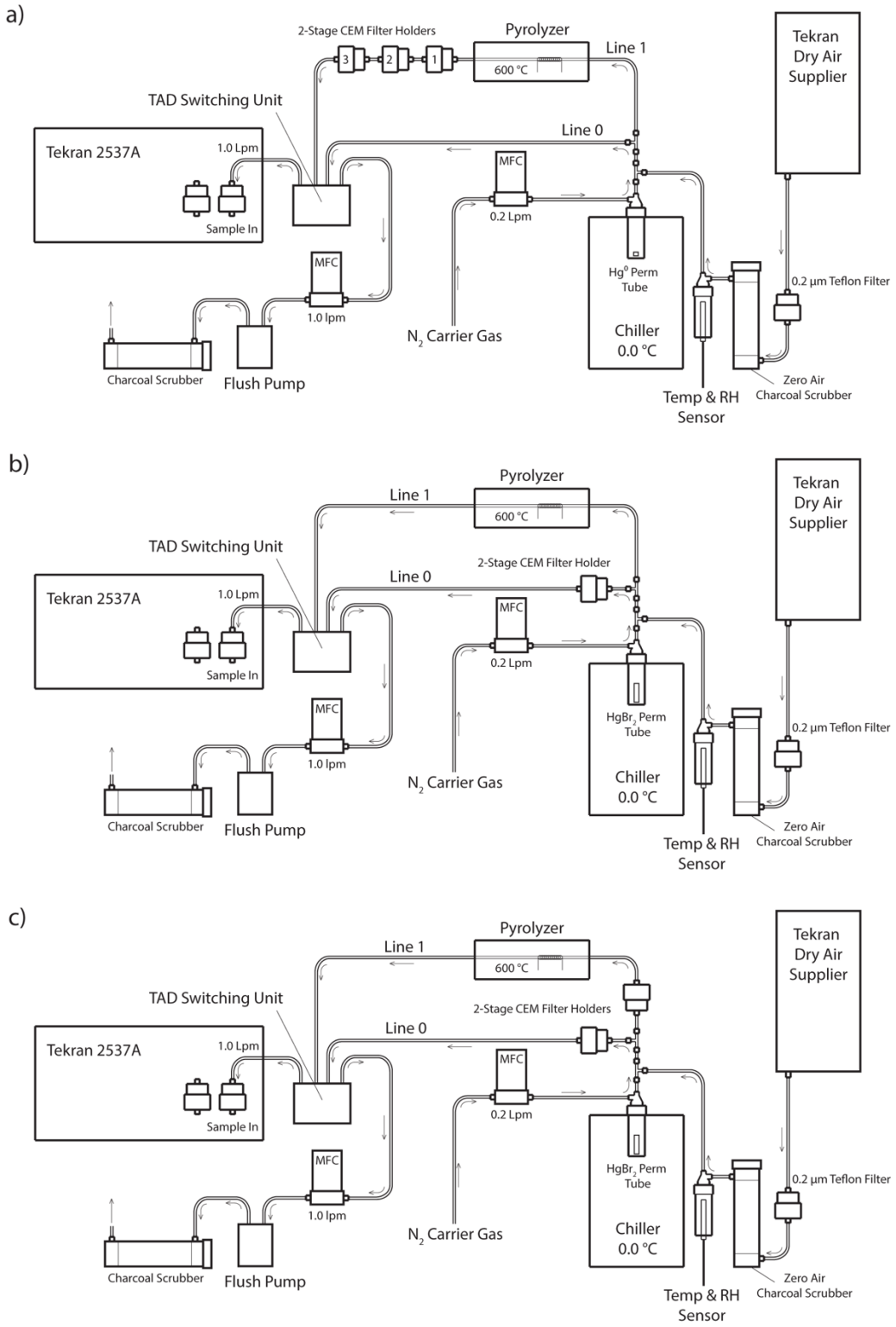

Figure 1. Schematic of the Hg vapor permeation system configurations for: a) GEM permeations b) $HgBr_2$ permeations c) Simultaneous $HgBr_2$ loading on two sample lines. Note dry air supplier disconnected for ambient and elevated humidity $HgBr_2$ permeations, with sample path starting at 0.2 µm Teflon particulate filter and water bath inserted immediately in front of the charcoal scrubber. All tubing is PTFE, except for the quartz glass pyrolyzer tube and PFA filter holders.

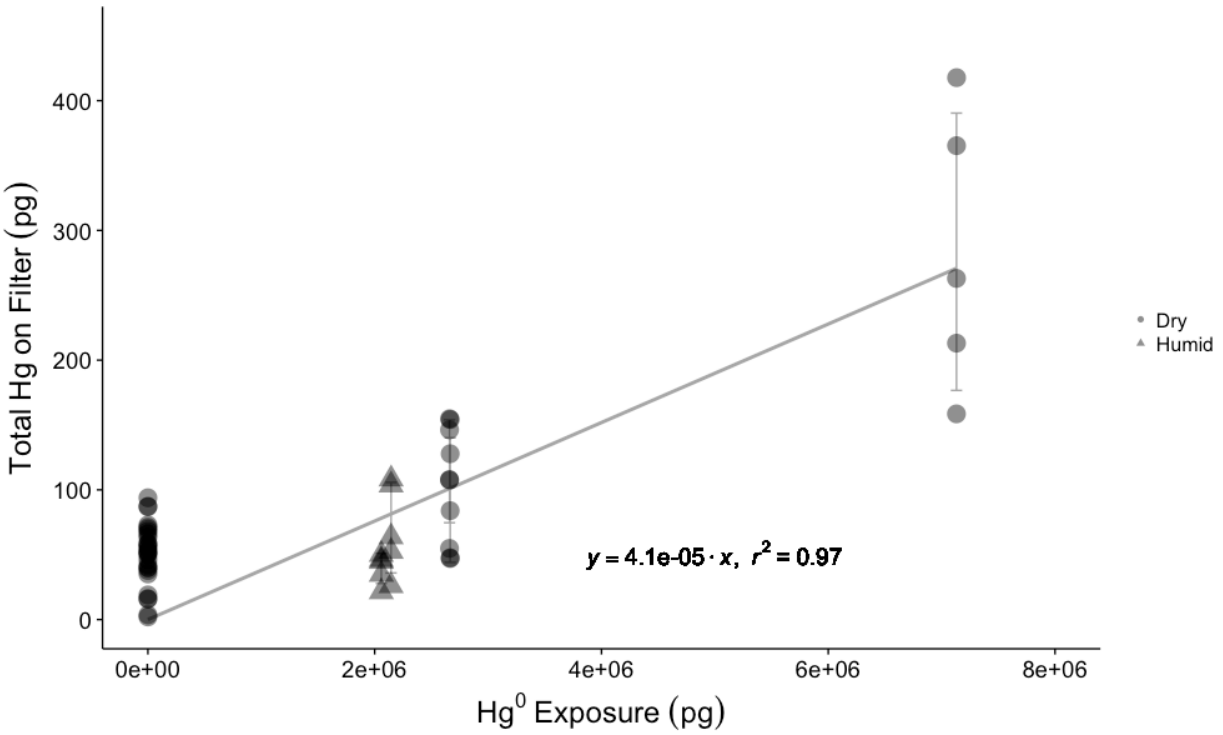

542

543 **Figure 2.** Total Hg recovered on CEM material for blank filters (Hg exposure = 0 pg) and different Hg^0 vapor
544 permeations in dry (0.5 ± 0.1 g m^{-3} WV) and humid air (2-4 g m^{-3} WV). Circles represent dry air permeations,
545 triangles represent humid air exposures, and all permeation exposures were blank-corrected. The regression line
546 shows the relationship between total Hg^0 exposure and blank-correct mean total Hg recovered on CEM filters (error
547 bars ± one standard deviation), with a slope of $4.1x10^{-5}$ indicating a linear uptake rate of 0.004%.

548

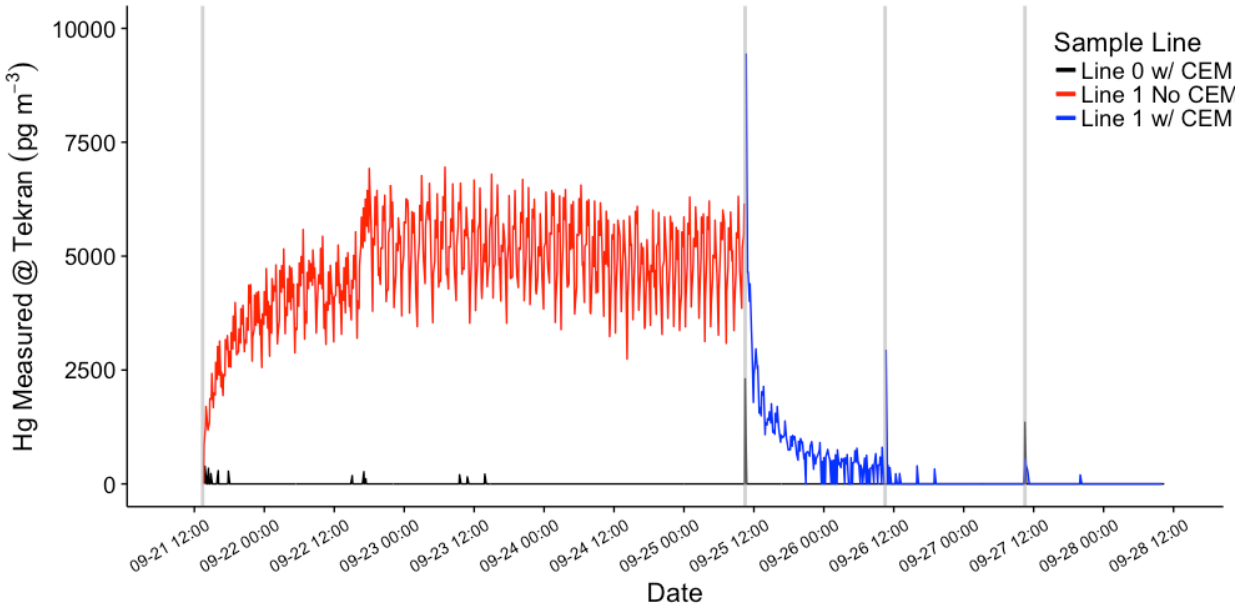

Figure 3. $HgBr_2$ permeations in clean dry lab air using the configuration in Figure 1B (red line) and Figure 1C (blue line). The red line indicates total Hg released from permeation tube and passing through pyrolyzer on Line 1 before being measured by Tekran 2537A, black line indicates Hg reaching 2537A through CEM filters on Line 0. Vertical grey lines indicate open system during filter deployments.

Table 1.

Sample	Start	End	Sample Time (min)	Sample Flow (lpm)	Sample Volume (m^3)	Total Hg on CEM (pg)	Blank Correct (pg)	Total Hg @ Tekran (pg)	A to B Filter Brkthru (%)
Mean CEM Filter Blank							54		
					Clean Dry Air (0.3 ± 0.05 g m^{-3} wv)				
HgBr 1P	*9/21/17 13:25*	*9/25/17 10:25*	*5580*	*1.00*	*5.580*	*na*	*na*	*25181*	*na*
HgBr 1A	9/21/17 13:25	9/25/17 10:25	5580	1.00	5.580	49478	49424	15	0.10
HgBr 1B						101	47		
HgBr 2A	9/25/17 10:30	9/26/17 10:30	1440	1.00	1.440	8901	8847	0	0.20
HgBr 2B						71	17		
HgBr 3A	*9/25/17 10:30*	*9/26/17 10:30*	*1440*	*1.00*	*1.440*	*9125*	*9072*	*1155*	*0.36*
HgBr 3B						*86*	*33*		
HgBr 4A	9/26/17 10:40	9/27/17 10:25	1425	1.00	1.425	8494	8440	0	0.28
HgBr 4B						77	24		
HgBr 5A	*9/26/17 10:40*	*9/27/17 10:25*	*1425*	*1.00*	*1.425*	*8306*	*8253*	*10*	*0.36*
HgBr 5B						*83*	*29*		
HgBr 6A	9/27/17 10:35	9/28/17 10:25	1430	1.00	1.430	8496	8442	0	0.22
HgBr 6B						72	19		
HgBr 7A	*9/27/17 10:35*	*9/28/17 10:05*	*1410*	*1.00*	*1.410*	*8386*	*8333*	*6*	*0.15*
HgBr 7B						*66*	*13*		
					Clean Humid Air (4.4 ± .2 g m^{-3} wv)				
HgBr H1P	*10/2/17 16:10*	*10/3/17 15:20*	*1390*	*1.00*	*1.390*	*na*	*na*	*5888*	*na*
HgBr H1A	10/2/17 16:10	10/3/17 15:20	1390	1.00	1.390	10498	10444	1700	0.25
HgBr H1B						80	27		
HgBr H2A	10/3/17 15:30	10/4/17 14:40	1390	1.00	1.390	8589	8535	164	0.13
HgBr H2B						65	11		
HgBr H3A	*10/3/17 15:30*	*10/4/17 14:40*	*1390*	*1.00*	*1.390*	*8182*	*8129*	*420*	*0.54*
HgBr H3B						*98*	*44*		
HgBr H4A	10/4/17 14:50	10/5/17 11:50	1260	1.00	1.260	7504	7451	0	0.31
HgBr H4B						76	23		
HgBr H5A	*10/4/17 14:50*	*10/5/17 11:50*	*1260*	*1.00*	*1.260*	*7576*	*7522*	*25*	*0.25*
HgBr H5B						*73*	*19*		
HgBr H6P	*10/5/17 12:05*	*10/9/17 10:25*	*5660*	*1.00*	*5.660*	*na*	*na*	*11889*	*na*
HgBr H7A	10/9/17 10:40	10/10/17 10:45	1445	1.00	1.445	9024	8970	105	na
HgBr H7B						2672*	2618*		
HgBr H8A	*10/9/17 10:40*	*10/10/17 10:45*	*1445*	*1.00*	*1.445*	*12359*	*12305*	*397*	*na*
HgBr H8B						*75*	*21*		
					Clean High Humidity Air (10.9 ± 1.7 g m^{-3} wv)				
HgBr H9A	10/10/17 10:50	10/11/17 9:30	1360	1.00	1.360	10920	10866	181	0.22
HgBr H9B						78	24		
HgBr H10A	*10/10/17 10:50*	*10/11/17 9:30*	*1360*	*1.00*	*1.360*	*11413*	*11359*	*308*	*0.00*
HgBr H10B						*53*	*0*		
HgBr H11A	10/11/17 9:35	10/12/17 9:35	1440	1.00	1.440	12001	11947	5	0.00
HgBr H11B						52	0		
HgBr H12A	*10/11/17 9:35*	*10/12/17 9:35*	*1440*	*1.00*	*1.440*	*12579*	*12525*	*40*	*0.29*
HgBr H12B						*90*	*36*		
HgBr H13P	*10/12/17 9:40*	*10/13/17 9:40*	*1440*	*1.00*	*1.440*	*na*	*na*	*1430*	*na*
HgBr H13A	10/12/17 9:40	10/13/17 9:40	1440	1.00	1.440	13152	13099	4	0.12
HgBr H13B						69	16		

Table 1. Summary of CEM filter loading and breakthrough during $HgBr_2$ permeations. Samples denoted P indicate approximate permeation rate check through Line 1 via pyrolyzer and Tekran 2537A, italicized text indicates filter deployments on Line 1, and * indicates high values due to leak around first filter seal.